Friction Estimation at Tire-Ground Contact

Johannes Edelmann
Technische Universität Wien

Massimiliano Gobbi and Giampiero Mastinu
Politecnico di Milano

Manfred Ploechl
Technische Universität Wien

Giorgio Previati
Politecnico di Milano

1. INTRODUCTION

A number of highly qualified papers that address the estimation of the friction at tire-ground interface can be found in the literature. Over the past ten years of research, the focus remains on the following topics [1]:

1. Enhancement of the active safety of vehicles and reduction of road accidents
2. Driver warning the available friction
3. Broadcasting of the road surface friction condition (info for vehicle drivers or traffic info centers)
4. Enhanced road maintenance
5. Traffic management

A comprehensive research is reported in [1] where a number of different technologies are compared referring to friction estimation.

Basically there are four different strategies for friction estimation, which are based on

1. physical vehicle models
2. force measurement
3. vision
4. data fusion

A comprehensive overview of the literature produced on road friction estimation is out of the scope of this paper. We cite a limited number of recent papers belonging to the four addressed groups.

1. Physical vehicle models [1,5,17] are prone to the uncertain vehicle parameters and cannot detect properly friction at each single wheel. Nonetheless they can provide some enhancement with respect to the normal situation in which the driver uses mainly his/her inspection (of the road surface) and steering wheel torque as the (fuzzy) data to estimate friction.
2. Force measurement [1,2,3,4,16] seems a very promising way of detecting tire-road friction, provided that the sensors and the procedures are robust and signal to noise ratio is sufficiently low. Our paper belongs to this group of research and aims to overcome the addressed problems.
3. Vision can be a very effective way of estimating friction [1] but some additional efforts for reducing costs seems necessary. One major vision is estimating the friction that the wheel experiences earlier. This is quite important.
4. Mixing all the information available could be a viable (and cheap) way to estimate friction, however the accuracy strongly depends on which and how information is used, (see e.g. [6,7]).

The paper deals with a brief description of the smart wheel that has been used to measure the forces at tire-ground interface. Then the maneuvers providing the forces and moments at the rear wheel of a reference vehicle are reported. Finally, the algorithm used to detect the friction potential is presented and applied.

2. SMART WHEEL

The concept design of the developed smart wheel for measuring forces and moments is shown in Fig. 1 ([8, 9, 10, 11, 12, 13, 14]). The three spoke structure, supporting the central part of the wheel, is constrained at the rim by means of three sliding spherical joints. Such a structure is statically determined and so it is quite easy to find the forces acting at the hub if the forces acting at the spoke tips (i.e. at the constraints) are measured. Due to the nature of the constraints (sliding spherical joints) only two forces in two orthogonal directions are acting at each spoke tip, so the force measurement is simple. The proof that the three spoke structure is statically determined is shown in Fig. 1. Actually Fig. 1 shows that the two constraints at two adjacent cantilevers/spokes (e.g. joints 1, 3) are equivalent to the virtual rotational joint (1+3). So the three spoke structure is equivalent to a simply supported beam, the simplest statically determined structure.

The joints must be frictionless and so they have been designed as laminas located between each spoke tip and the rim (Fig. 2). The shape of the laminas has been optimized in order to reproduce a sliding spherical joint, i.e. a joint with very high axial and tangential stiffness and with very low radial stiffness (the addressed directions are given referring to the wheel). Additionally, the lamina allows rotations around the tangential direction and the axial direction. The rotation around the spoke axis is provided by a proper compliant cross shape of the spoke. Finally, to eliminate friction a quasi-statically determined structure is obtained, since the tip of each spoke is connected to the rim by means of an elastic joint (joints 1, 2, 3 in Fig. 1).

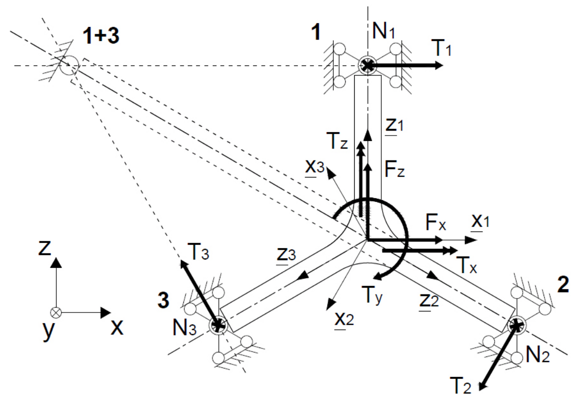

Figure 1. Concept design of the smart wheel.

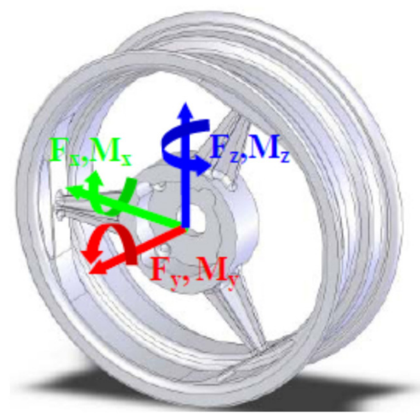

Figure 2. Actual structure of the smart wheel. The three sliding spherical joints at the three spoke tips are realized by means of three laminas.

The three spoke structure can be instrumented by means of 12 strain gauges at the positions shown in Fig. 3 and connected in half-bridge configuration. Their positions have been defined in order to maximize the output (voltage) of the strain gauges for all combinations of loads applied at the wheel center. The strain gauges resistance is 350 Ω, sufficiently high to reduce the power consumption. The strain gauges are intentionally located in the area where the bending moments acting at each spoke produce high strains. In Fig. 4 the measuring wheel mounted on the reference car is shown. The performance of the smart wheel is reported in Tab 1.

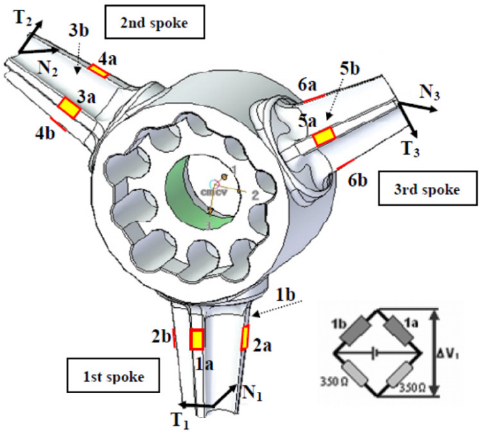

Figure 3. Location of the 12 strain gauges.

Table 1. Measuring wheel technical

Maximum force	F_x, F_y, F_z	15	kN
Uncertainty 95%		0.5	% F.S.
Resolution		±1	N
Maximum torque	M_x, M_y, M_z	3.5	kNm
Uncertainty 95%		0.3	% F.S.
Resolution		±0.2	Nm
Cross-talk		<±2.0	%
Acquisition frequency		200	Hz

3. TEST MANEUVERS

A reference vehicle has been taken into consideration for simulating the running of actual vehicles along public roads. A series of manoeuvres have been performed on (dry or wet) asphalt surface at the Politecnico di Milano referring to the vehicle in Fig. 4, whose data are reported in Tab 2.

Figure 4. Smart wheel and the reference car used for friction estimation.

Table. 2. Measuring wheel specifications.

Mass	1300	kg
Wheel base	2.552	m
Centre of gravity distance from front axle	1.05	m
Track	1.56	m
Tire radius	0.313	m
Yaw moment of inertia	2050	kgm^2
Tire	205/60 R15	

The manoeuvers are

- steering ramp at approximately 30 km/h
- straight running, applying parking brake ramp from approximately 30 km/h
- steering ramp (spiral) plus parking brake ramp from approximately 30 km/h

The first two manoeuvres have been conceived to test the estimation algorithm in condition of pure lateral or longitudinal slips, respectively. The third manoeuvre is proposed to test the algorithm efficiency in case of combined longitudinal and lateral slip.

In Fig. 5, 6, 7 the longitudinal and lateral forces and the self-aligning torque on the measuring wheel are reported for the considered manoeuvres.

The contact forces of the rear right tire are considered and reported in the following figures.

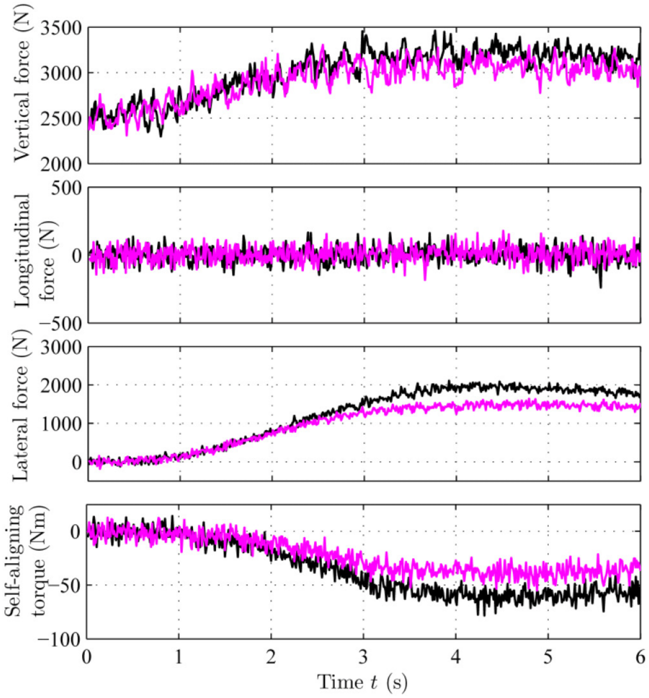

Figure 5. Steering ramp maneuver. Black line: dry asphalt. Magenta line: wet asphalt.

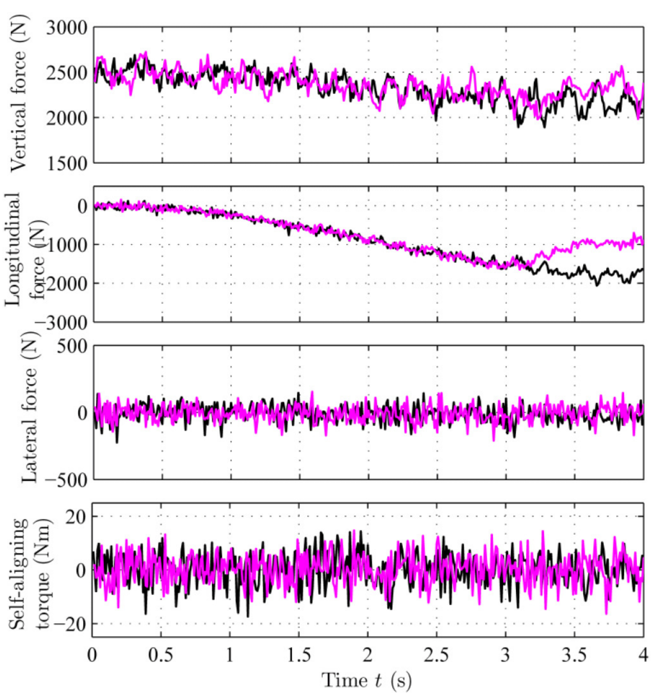

Figure 6. Straight running maneuver. Black line: dry asphalt. Magenta line: wet asphalt.

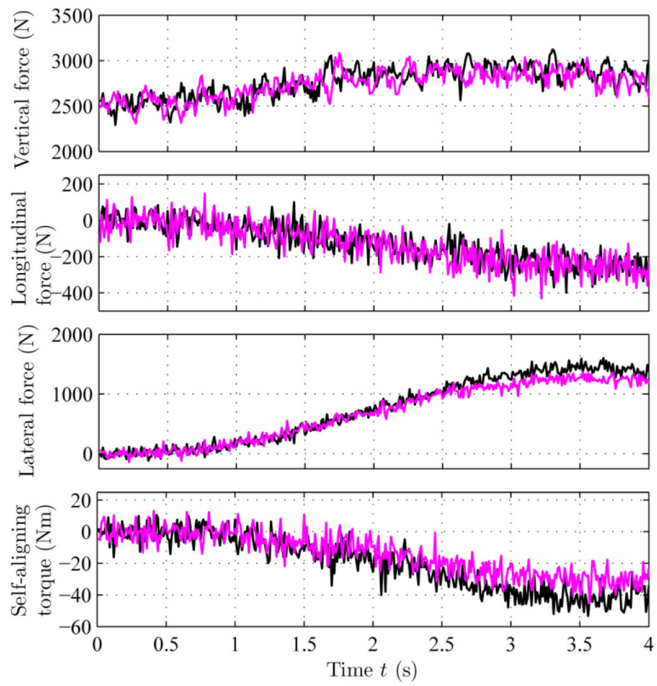

Figure 7. Steering ramp plus parking brake ramp (combined lateral and longitudinal slips). Black line: dry asphalt. Magenta line: wet asphalt.

No sensors other than the smart wheel were fitted into the car. The actual friction of the running surface has been estimated (by a proper procedure) and reported in Tab. 3.

Table 3. Estimated friction coefficients at the running surface.

Rear smart wheel	Dry asphalt	Wet asphalt
longitudinal	1.0-1.1	0.6-0.7
lateral	0.8-0.9	0.5-0.6

4. FRICTION ESTIMATION

Estimation of the friction coefficient in up-to-date vehicle application is generally based on sensing the vehicle response to driver input from steering, braking or accelerating. The mathematical algorithm is then typically based on a mathematical model to represent vehicle and tire dynamics and on some kind of Kalman-filter or RLS approach. As a consequence, some time lag of the estimated maximum friction level can be observed [17].

Pure longitudinal friction coefficient estimation usually depends on the quality of the longitudinal slip estimation, which is particularly difficult to estimate if the transferred moments from (friction) brakes or 4WD are not known exactly. The availability of this moment together with the longitudinal tire force F_x and the wheel load F_z considerably improves the quality of estimation.

Similarly, pure lateral friction coefficient estimation relies on lateral vehicle and tire dynamics, i.e. sideslip angle of the vehicle and lateral tire force estimation, which is complicated due to their mutual interrelations with respect to external disturbances such as cross gradient of the road or side wind gusts. Estimation of a combined maximum friction levels has been rarely addressed in literature so far.

The applied estimation methods perform well, as long as demanded tire forces are close to their respective saturation level. The fact that the self-aligning moment saturates at smaller sideslip angles than the lateral tire force, exemplarily shown in Fig. 8, motivated a number of researchers to incorporate the relation between self-aligning moment and lateral friction coefficient in their friction potential estimation methods, e.g. [3, 4, 5]. The drawback of the need for an observer to estimate the self-aligning moment (and sideslip angle) [4], has been relieved with the introduction of Electric Power Assisted Steering (EPAS), which provides reliable estimates of the rack force. The problem to allocate the rack force to separate self-aligning moments for both tires of the front axle, taking non-linear geometric and elastic properties of the suspension system as well as individual tire forces in longitudinal, lateral and vertical direction into account, can be completely alleviated by making use of the proposed smart wheel. The direct and immediate availability in particular of the self-aligning moment and all tire forces allows for an immediate estimation of the maximum lateral friction level. Additionally, when using additional sensors for vehicle states, the complete tire characteristics adapted to the actual road surface may be identified online. An immediate estimate of the maximum lateral friction level can be obtained from evaluating the unique relation between lateral tire force, self-aligning moment, sideslip angle and lateral friction coefficient combined in the Gough-plot, Fig. 9. The idea to use the Gough-plot for lateral friction potential estimation has already been clearly developed in [2].

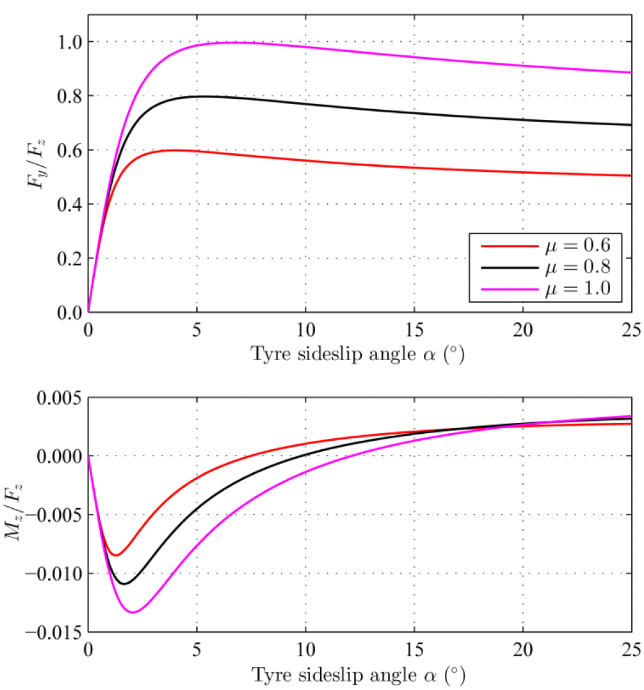

Figure 8. Normalized lateral tire force and aligning moment depending of varied lateral friction coefficients.

An exemplary Gough-plot in Fig. 9 depicts the lateral tire force F_y versus the self-aligning moment M_z, both normalized for the vertical load F_z, for various sideslip angles α and lateral friction coefficients μ utilizing a steady-state tire force model. Solid lines mark constant lateral friction coefficients, dashed lines constant sideslip angles. It is shown in [2] for the brush tire model, that for the case of partial sliding in the contact patch area, a pair of values [F_y, M_z] corresponds to a unique pair of values [α, μ] which is the principle of maximum lateral friction level estimation here as well. For small sideslip angles, and thus mostly adhesion in the contact patch area, the lines of constant lateral friction coefficient almost coincide, and the lateral friction coefficient cannot be estimated. This becomes also clear from the linear increase of lateral tire force and self-aligning moment, respectively, for small side slip angles independent of the lateral friction coefficient in Fig. 8.

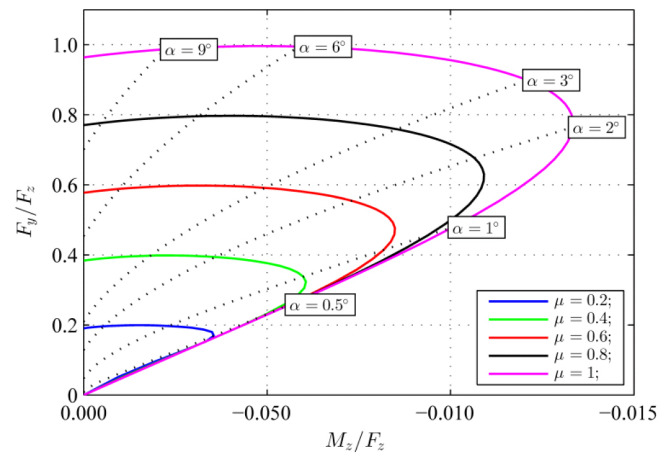

Figure. 9. Gough-plot referring to Fig. 8.

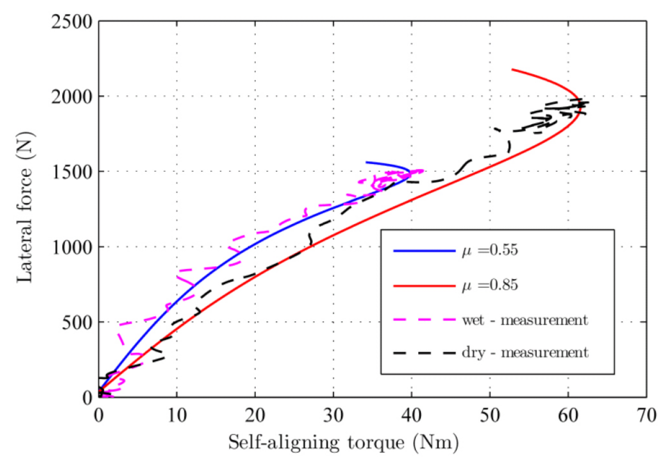

Figure 10. Gough-plot referring to steering ramp maneuvers in Fig. 5.

Fig. 10 illustrates an extract of the Gough-plot related to the specific tire of the test vehicle and the measured data from the smart wheel, dashed lines, from the steering ramp maneuver on dry and wet asphalt referring to Fig. 5. The solid lines are derived applying a simplified Magic Formula tire model, [15], based on a nominal set of tire parameters (e.g. from test rig parameterization; μ_0=1, F_z=3000 N). Load and lateral friction level coefficient different from nominal may either be accounted for in the tire model itself or by applying the similarity method, [2,15]. Effects from tire camber angle and tire relaxation are not considered here, but might be in particular important at (this) low speed maneuver and contribute to the observed difference. At moderate and higher speeds however, the latter effects can be neglected.

The mapping between the lateral friction coefficient μ and [F_y, M_z] has been derived off-line for quick on-line estimation with a look-up table. To better demonstrate the immediate lateral friction estimation the estimator has been turned on at about t=2 s starting from μ_0=1, Fig. 11. While on dry asphalt the lateral excitation level is yet high enough (only 20% of saturated levels) to immediately adapt to the lower maximum lateral friction level; more time is required on wet asphalt.

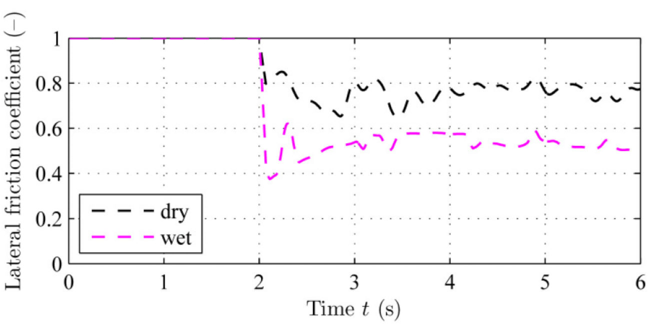

Figure 11. Lateral friction coefficient estimation referring to steering ramp maneuvers in Fig. 5.

Extending the two-dimensional Gough-plot and the corresponding look-up table by the longitudinal tire force F_x, relaxes the restriction to pure slip conditions. In this way it is possible to estimate the (pure) lateral friction coefficient even when longitudinal slip (due to braking/accelerating) is present. For a moderately applied parking brake corresponding to a final longitudinal tire force of about 300 N during the steering ramp maneuver, shown in Fig. 12, about the same lateral friction coefficient has been estimated as for steering ramp without longitudinal slip shown in Fig. 11.

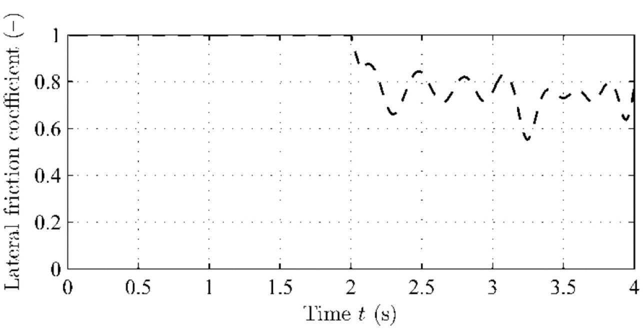

Figure 12. Lateral friction coefficient estimation referring to steering ramp maneuver in Fig. 7 on dry asphalt with applied parking brake.

The estimation of the longitudinal friction coefficient is typically based on a Kalman-filter or RLS approach facilitating additional measurements, such as rotational wheel speed and longitudinal acceleration, for longitudinal slip estimation. Then, longitudinal tire characteristics are processed to directly identify the maximum friction level or indirectly from the slip stiffness, which is assumed to depend on the friction coefficient. These methods benefit in particular from measured data of the longitudinal and vertical tire force and the driving or braking moment of the smart wheel.

For immediate longitudinal friction coefficient estimation only the longitudinal tire characteristics are processed (from given longitudinal slip) to reveal the different maximum friction levels in longitudinal and lateral direction, Fig. 13. Note, this method is not robust with respect to uncertainties in measured data and variable parameters of the tire model. However, applying the above methods is straight-forward and will relieve the situation presuming sufficient longitudinal excitation.

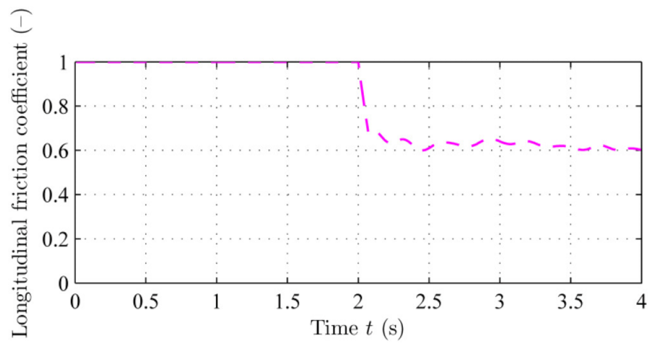

Figure 13. Longitudinal friction coefficient estimation referring to straight running maneuver in Fig. 6 on wet asphalt with applied parking brake.

5. SUMMARY/CONCLUSIONS

The proper estimation of the friction potential between the tires of a vehicle and varying conditions of the road surface is still an unsolved challenge in vehicle dynamics. The solution of the problem will contribute not only to increase the active safety of our vehicles; but can also help to further improve vehicle performance and increase efficiency regarding energy consumption. The present paper proposes a simple solution based on a smart wheel, which is able to measure the three forces and three moments acting at the hub the wheel.

A number of maneuvers representing the actual running behavior of vehicles on public roads have been performed. The considered running conditions refer to pure lateral and longitudinal dynamics, but also manoeuvres involving combined lateral and longitudinal tire slip have been performed to account for the mutual influence of lateral and longitudinal tire forces. The maximum friction level has been estimated in lateral direction based on the evaluation of the Gough-plot, which gives a unique map of the self-aligning torque with respect to the lateral force of the tire as a function of the maximum (lateral) friction level. The method allows to estimate a lateral friction coefficient without delay.

Incorporating the self-aligning torque in the estimation method, without the need to account for suspension geometry and sideslip angle estimation due to application of the smart wheel, requires only low lateral slip excitation. The Gough-plot is extended by the longitudinal tire force to derive a pure lateral friction coefficient despite longitudinal slip. In a similar way, the longitudinal tire characteristics are processed to estimate the longitudinal friction coefficient from measured data of the smart wheel, not considering the estimation of the longitudinal slip in this paper.

As the applied methods are based on a ("Magic Formula"-type) tire model, the estimation is expected to be sensitive to a number of tire parameters, such as inflation pressure or tire wear, which holds true for up-to-date model based maximum friction level estimators in general.

REFERENCES

1. Andersson, M., et al., "Road Friction Estimation", IVSS Project Report, Ref.-Nr. 2004:17750, 2007, http://www.ivss.se/upload/IVSS_2004-17750_final_report_070608.pdf
2. Pasterkamp, W., "The Tire As Sensor To Estimate Friction," Doctoral Dissertation of TU Delft, Delft University Press, 1997. ISBN 90-407-1538-6
3. Gerdes, J.Ch. and Hsu, Y.-H.J., "The Predictive Nature of Pneumatic Trail: Tire Slip Angle and Peak Force Estimation using Steering Torque," 9th Int. Symposium on Advanced Vehicle Control (AVEC), Kobe, Japan, 2008.
4. Takagi, F. and Inoue, N., "An Estimation Method of the Maximum Tire-road Friction Coefficient Using an Electric Power Assist Steering," 10th Int. Symposium on Advanced Vehicle Control (AVEC), Loughborough, UK, 2010.
5. Ahn, C., Peng, H., Tseng, E., "Robust estimation of road friction coefficient using lateral and longitudinal vehicle dynamics," Vehicle System Dynamics 50:6, 961-985, 2012.
6. Kobalka U et Al, "Optimization of sensor configuration with respect to RMSE and costs", International Munich Chassis Symposium, ATZ, 2014
7. Petry F et Al, "Tyre road interaction: a multi-scale journey form rubber friction", International Munich Chassis Symposium, ATZ, 2014
8. Gobbi, M. and Mastinu, G., "Wheels with Integrated Sensors for Measuring Tire Forces and Moments," 7th International Symposium on Advanced Vehicle Control (AVEC), Arnhem, The Netherlands, 2004.
9. Gobbi, M., Mastinu, M., Rocca, G., "Design of a Smart Wheel," Proc. of the 2008 Int. Design Engineering Technical Conference, IDETC2008-49838, New York, USA, 2008. ISBN 0-7918-3831-5
10. Gobbi, M., Mastinu, M., Rocca, G., "A smart wheel for improving the active safety of road vehicles," Proc. of the 2010 Int. Design Engineering Technical Conference IDETC 2010, IDETC2010-29059, Montreal, Canada, 2010.
11. Gobbi, M., Mastinu, G., Giorgetta, F., "Sensors for measuring forces and moments with application to ground vehicle design and engineering," Proc. ASME IMECE, 2005.
12. Gobbi, M., Previati, G., Mastinu, G., "Refinement design of a measuring wheel," Proc. ASME DETC2011, Washington, DC, USA, 2011.
13. Mastinu, G., Gobbi, M., Previati, G., "A new six-axis load cell," Part I: Design, Exp. Mech. 51 (3), 373-388, 2011. DOI:10.1007/s11340-010-9355-1.
14. Gobbi, M., Previati, G., Guarneri, P., Mastinu, G., "A new six-axis load cell," Part II: error analysis, construction and experimental assessment of performances, Exp. Mech. 51 (3), 389-399, 2011. DOI:10.1007/s11340-010-9350-6.
15. Pacejka, H., "Tire and Vehicle Dynamics," Butterworth-Heinemann, 2012.
16. Xiong, Y., Zhuang, Y., Tuononen, A., "Assessment of Brush Model Based Friction Estimator Using Lateral Vehicle Dynamics," 12th International Symposium on Advanced Vehicle Control (AVEC), Tokyo, Japan, 2014.
17. Cheli, F. and Sabbioni E., "Effect of cornering forces measurement on real-time estimation of tyre-road friction coefficient, vehicle sideslip angle and road bank angle," 12th International Symposium on Advanced Vehicle Control (AVEC), Tokyo, Japan, 2014.

CONTACT INFORMATION

prof dr-ing Giampiero Mastinu
mastinu@mecc.polimi.it

Prof. Dr.techn. Manfred Plöchl
m.ploechl@tuwien.ac.at

ACKNOWLEDGMENTS

Dr Mario Pennati of the Laboratory for the Safety of Transport System is gratefully acknowledged for having performed the experimental activities. The research has been funded by the National Project ITS Italy 2020, Ministry of the Research, Italy.